MYCOTAXON

ISSN (print) 0093-4666 (online) 2154-8889 Mycotaxon, Ltd. ©2022

January–March 2022—Volume 137, pp. 123–134

https://doi.org/10.5248/137.123

New Turkish records of *Hebeloma excedens* and *H. geminatum*, and confirmation of *H. celatum*

Ayten Dizkirici[1], Aysenur Kalmer[1], İsmail Acar[2*]

[1] *Department of Molecular Biology and Genetics, Van Yüzüncü Yıl University, 65080, Van, Turkey*

[2] *Department of Organic Agriculture, Başkale Vocational High School, Van Yüzüncü Yıl University, 65080, Van, Turkey*

* Correspondence to: *iacar2011@gmail.com*

Abstract—*Hebeloma excedens* and *H. geminatum* are reported as new records and *H. celatum* is confirmed for the Turkish mycota, on the basis of morphological and phylogenetic data. Morphological descriptions, illustrations, and comparisons with closely related taxa are provided.

Key words—*Agaricales*, *Basidiomycota*, *Hymenogastraceae*, ITS, phylogeny

Introduction

Hebeloma (Fr.) P. Kumm. (*Hymenogastraceae, Agaricales*) is a genus of ectomycorrhizal and mostly poisonous basidiomycetes primarily distributed in temperate, boreal, arctic, and alpine habitats (Vesterholt 2005, Beker & al. 2016, Cripps & al. 2019). The genus is characterized by a mostly two coloured convex to plano-convex pileus, dull brown lamellae, presence of a veil, and morphologically distinctive cheilocystidia (Beker & al. 2016).

Identification of *Hebeloma* at the species level is considerably challenged by morphological similarities and infrequent or transient characters (Eberhardt & al. 2012). Therefore, species determination and classification and their phylogenetic relationships within the genus have come to rely upon DNA genomic sequences such as the nuclear ribosomal DNA internal

transcribed spacer (nrDNA ITS) region. One advantage of selecting the ITS region for analysis is the many *Hebeloma* sequences available in GenBank. Moreover, the availability of universal primers, high rate of PCR success, and superior resolution at infrageneric levels are other important advantages of the ITS region (Aanen & al. 2000, 2001; Vesterholt & al. 2014; Eberhardt & al. 2015a,b).

Twenty-eight *Hebeloma* species have been recorded from Turkey (Sesli & Denchev 2014; Güngör & al. 2015; Sesli & al. 2015, 2018; Solak & al. 2015; Doğan & Kurt 2016; Dizkirici & al. 2019). Beker & al. (2016) investigated seven Turkish specimens (representing six species, including *H. celatum* and *H. subtortum*) using molecular data but did not provide morphological details; subsequently Dizkirici & al. (2019) provided detailed descriptions of Turkish *H. subtortum*. *Hebeloma celatum,* which has been widely reported from Europe, known from Turkey only by a single 2008 collection from Adana province (Grilli & al. 2015). Here, we provide full descriptions and phylogenetic results for *Hebeloma excedens*, *Hebeloma geminatum*, and *Hebeloma celatum*.

Hebeloma excedens is placed in *H.* sect. *Hebeloma,* characterized by the visible cortina seen in young basidiomes and cheilocystidia that are always lageniform or ventricose; *H. geminatum* belongs to *H.* sect. *Denudata,* characterized by cheilocystidia that are primarily clavate-stipitate or clavate-ventricose and basidiospores that are weakly dextrinoid; and *H. celatum* is placed in *H.* sect. *Velutipes,* characterized by a velutinate stipe, clavate cheilocystidia, strongly dextrinoid basidiospores, and absence of cortina (Vesterholt 2005, Beker & al. 2016, Grilli & al. 2015).

In the present study, we used morphological and ITS sequence analyses to identify *H. excedens* and *H. geminatum* as new Turkish records and confirm the existing Turkish record of *H. celatum*.

Materials & methods

Taxon sampling & morphological studies

Fresh basidiomata of *H. excedens*, *H. geminatum*, and *H. celatum* were collected during 2017–18 fieldwork in south-eastern Turkey. Collected specimens were photographed in situ using a Canon (EOS 60D) camera equipped with a Tokina 100 mm macro lens. Macromorphological characters were determined based on field notes and colour photographs of fresh fruiting bodies. Dried specimens were examined microscopically after sectioning and rehydration following procedures in Vesterholt (2005) and Beker & al. (2016). Structures were observed using a Leica DM500 research microscope and measured with the Leica Application Suite v.3.4.0.

The samples were dried and deposited as voucher specimens in the Fungarium of Van Yüzüncü Yıl University, Van, Turkey (VANF). Abbreviations include: x = average length × width and Q = length/width ratio of basidiospores calculated based on the number (n) of spores measured. At least 100 spores, 30 basidia, and cheilocystidia from four samples were measured in distilled water and Melzer's reagent for each specimen. Additional potentially diagnostic characters were abbreviated according to Vesterholt (2005) with "D" indicating the degree of basidiospore dextrinoidity in Melzer's, "P" the degree of loosening of the basidiospore perisporium in Melzer's, and "O" the degree of ornamentation on the basidiospore surface.

DNA isolation, amplification, sequencing

Genomic DNA was extracted and purified directly from dried basidiomata using a modified CTAB protocol (Doyle & Doyle 1987). The purity and quantity of extracted DNA were determined by using a NanoDrop2000c UV–Vis Spectrophotometer and 0.8% agarose gel electrophoresis. Isolated stock DNA was stored at –20°C prior for further studies.

Two different samples were amplified for each *Hebeloma* species to increase reliability of the sequences. DNA was amplified in 25 µl volume mixtures containing genomic DNA (10 ng/µl), 10X PCR Buffer, $MgCl_2$ (25 mM), dNTP mixture (10 mM), the primer pair (10 µM), Taq polymerase (5u/µl) and sterile water. The primer pair N-nc18S10 5′AGGAGAAGTCGTAACAAG3′ / C26A 5′GTTTCTTTTCCTCCGCT3′ (Wen & Zimmer 1996) was used to amplify the ITS1-5.8S-ITS2 region. Amplicons were checked in 1% TAE agarose gel stained with Gelred dye. The PCR products were sequenced with forward and reverse primers in an ABI 3730XL automated sequencer. Sequences generated in the current study were submitted to GenBank.

Sequence alignment and phylogenetic analysis

All sequence chromatograms were opened using Finch TV (http://www.geospiza.com/finchtv/) and checked for reading errors, using the Q-Quality value to assess the accuracy of each base. BLAST analysis was performed using the UNITE (http://unite.ut.ee/) and NCBI (http://www.ncbi.nlm.nih.gov/) databases. Following a preliminary BLAST search that supported our newly amplified sequences in *Hebeloma*, we prepared a combined dataset containing sequences scoring the greatest number of BLAST hits.

Sixty-three sequences representing different *Hebeloma* sections were downloaded from the database and aligned with the newly amplified sequences. The final alignment was trimmed, with the data retained for further phylogenetic analyses. *Galerina pruinatipes* (AJ585510) and *G. pseudocamerina* (AJ585508) were chosen as outgroup.

The nucleotide evolutionary model for phylogenetic analyses was determined using MEGA 6.0 (Tamura & al. 2013), with the model with the lowest BIC (Bayesian Information Criterion) score selected. MrBayes v.3.2.6 (Ronquist & al. 2012) was employed for Bayesian phylogenetic analysis using the Markov chain Monte Carlo (MCMC) method (Yang & Rannala 1997) under K2P model. Two independent runs

with 4 chains each were run for 2 million generations, with trees sampled every 1000 generations. Analyses continued until the average standard deviation of split frequencies was <0.01. A Bayesian inference 50% majority rule tree and posterior probability values were estimated from the samples after discarding the first 25% of sampled trees and viewed with Figtree (Rambaut 2010).

Taxonomy

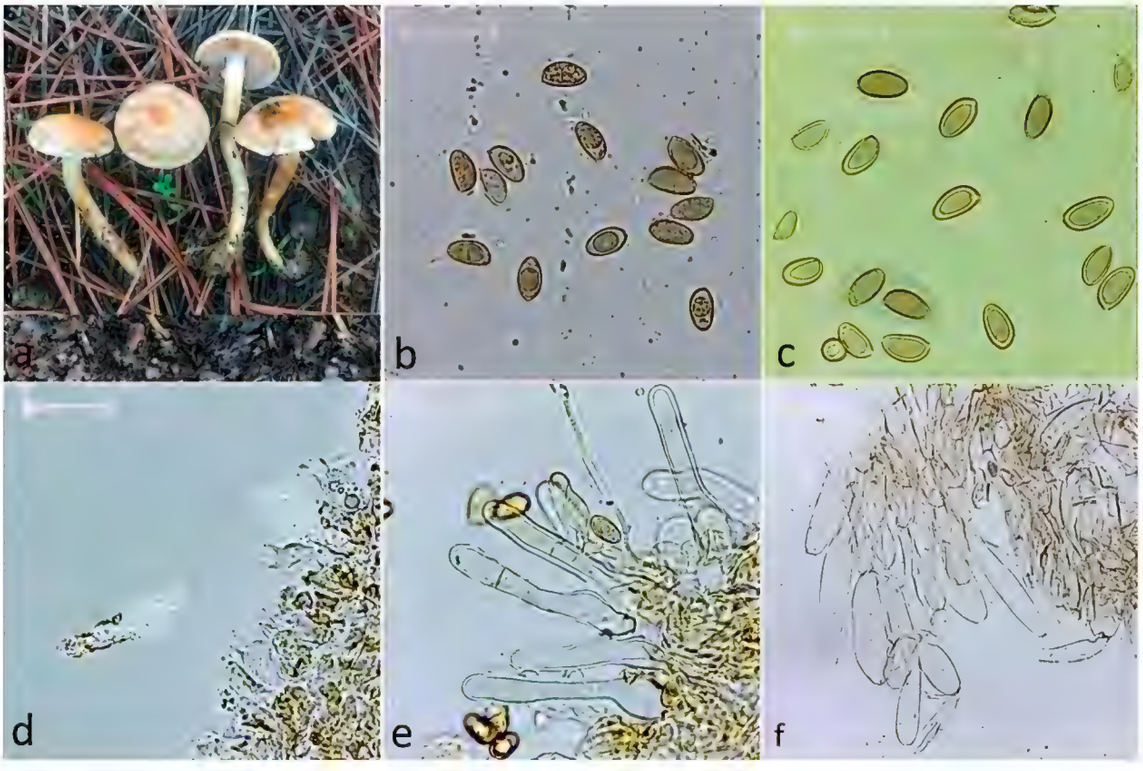

Fig 1. *Hebeloma excedens* [VANF1051]: a. Basidiomata; b. Basidiospores in distilled water; c. Basidiospores in Melzer's reagent; d. Basidia; e. Cheilocystidia; f. Pileipellis. Scale bars: a–e = 20 µm; f = 50 µm.

Hebeloma excedens (Peck) Sacc.,
Syll. Fung. 5: 806 (1887) Fig. 1

Pileus 15–25 mm, convex then almost flat and slightly umbonate, darker in the center (cocoa brown, yellow brown, or cream brown when young; later darkening), pale brown on most of the pileus, lighter at margin and with/without white velar remnants on the edges. Cortina present. Lamellae sinuate, subdecurrent, whitish cream when young, then pale brown, wider and eroded in age. Stipe 30–60 × 3–5 mm, cylindrical, equal, slightly curved, pale cream to light brown, pruinose above cortina zone, lower parts dirty and pale brown, with zones of brown fibrils.

Basidiospores 7.8–11(–12) × 4.1–6.3 µm, x = 9.8 × 5.2 µm, (n = 40; Q = 1.8–1.9), light yellow-yellow brown, elliptical, slightly ovoid, slightly roughened (O1), non- to slightly dextrinoid (D0; D1), perispore not loosening (P0). Basidia 19.7–31 × 7–9.8 µm, clavate, 4-spored. Pleurocystidia absent. Cheilocystidia 35–58 × 5–7 × 4.6–6.8 × 5.6–11 µm, ventricose, cylindrical apex, swollen at the base, rarely fully cylindrical, sometimes septate. Pileipellis an exocutis, ≤45 µm thick, slightly brownish, encrusted.

Specimen examined—**TURKEY, Bitlis, Van-Bitlis roadway**, under *Populus* sp., 38.3625°N 42.7614°E, 1952 m asl, 15.05.2018, Acar 1051 (VANF1051; GenBank MW544166, MW544167).

Hebeloma geminatum Beker, Vesterh. & U. Eberh., Persoonia 35: 122 (2015) Fig. 2

Pileus 25–110 mm, usually convex, occasionally umbonate or flattened, edges generally smooth, slightly incurved or wrinkled when young, when young sticky or moist, usually uniformly coloured (occasionally bi-coloured), cream to beige or (sometimes) light yellow, whitish toward margin. Cortina absent. Lamellae close, adnate to emarginate, notched, finely serrate at margin, droplets on margin when young or in humid conditions, color light pinkish-grey. Stipe 30–100 × 4–12 mm, flocculose, cylindrical to clavate (slightly swollen toward base), whitish.

Basidiospores 10–11.8 × 5.5–6.5 µm, x = 7.6 × 11.5 (n = 40; Q = 1.7–1.8), amygdaloid, non- to very slightly dextrinoid (D0,D1), ornamentation distinct

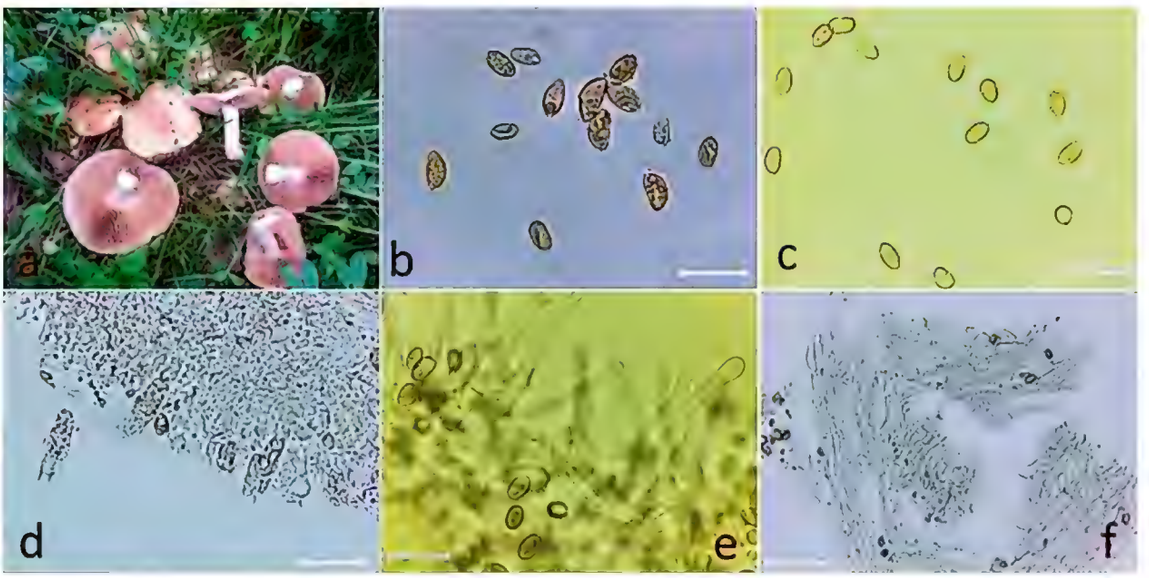

Fig 2. *Hebeloma geminatum* [VANF1116]: a. Basidiomata; b. Basidiospores in distilled water; c. Basidiospores in Melzer's reagent; d. Basidia; e. Cheilocystidia in Melzer's reagent; f. Pileipellis. Scale bars: a–e = 20 µm; f = 50 µm.

verrucose (O2,O3), perispore loosening (P0,P2). Basidia 31 × 8 µm, 4-spored (rarely 2-spored). Pleurocystidia absent. Cheilocystidia 50–85 × 7.2–11 × 4–5.6 × 3.3–4.5 µm, clavate-stipitate, spathulate, sometimes clavate-lageniform or sometimes capitate/bifurcate, septate, sinuate. Pileipellis an ixocutis; with a medium thick epicutis 110–180 µm thick, tramal hyphae beneath subcutis cylindrical, ellipsoid, sausage-shaped and inflating from septa ≤15 µm diam.

Specimen examined—**TURKEY, Bingöl, Elmalı village,** under *Populus* sp., 39.0256°N 40.7339°E, 1234 m, asl 20.05.2017, Acar 1116 (VANF1116; GenBank MW544168, MW544169).

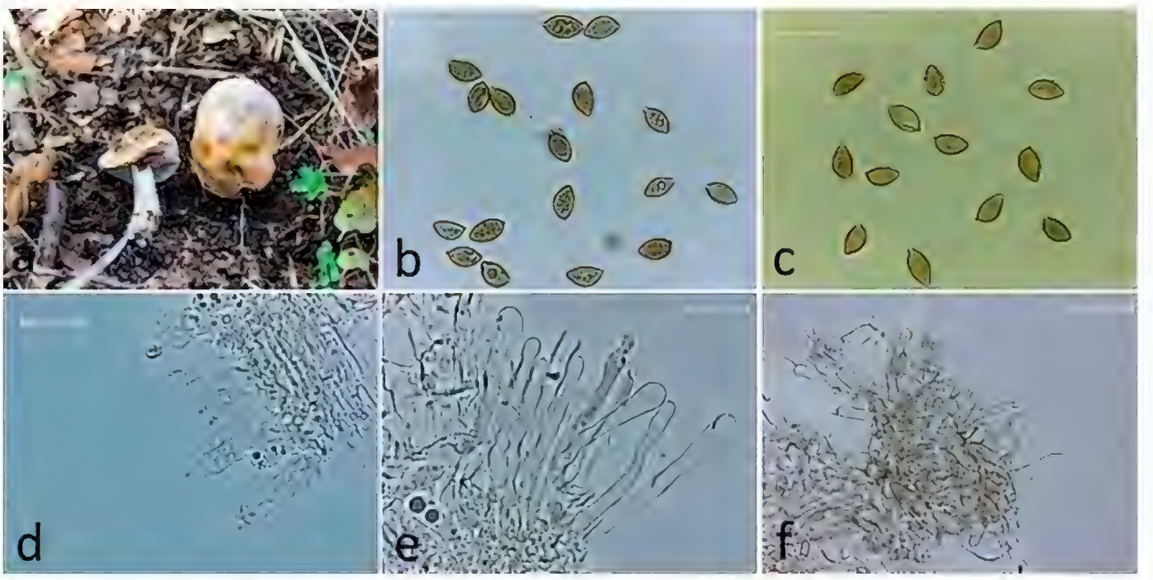

Fig 3. *Hebeloma celatum* [VANF1132]: a. Basidiomata; b. Basidiospores in distilled water; c. Basidiospores in Melzer's reagent; d. Basidia; e. Cheilocystidia; f. Pileipellis. Scale bars: a–e = 20 µm; f = 50 µm.

Hebeloma celatum Grilli, U. Eberh. & Beker,
Mycol. Progr. 15(5): 23. 2015 ["2016"] Fig. 3

Pileus 30–70 mm, convex, occasionally wrinkled, margin involute when young, sometimes smooth or wavy when mature, glutinous when damp, spotting variable, mono- or bi-coloured, cream, clay-buff, ochraceous or yellowish brown. Cortina absent. Lamellae adnexed to emarginate, white fimbriate margin usually present. Stipe 30–70 × 6–10(12) mm, white to light cream, surface with white powdery granules, fibrils, or floccules; cylindrical, clavate with bulbous base, rarely tapering, stuffed when young, later hollow.

Basidiospores 9–15.2 × 5.5–8.5 µm, x = 11.3 × 5.2 µm, (n = 40; Q = 1.6–1.8), amygdaloid, limoniform, yellow, yellowish brown, light yellow, reddish yellow to brown, apiculus distinct, guttulate, ornamentation distinct

verrucose (O2–O4), strongly dextrinoid (D2–D4), perispore loosening (P0–P2). Basidia 25–38 × 7–9.8 µm, cylindrical or clavate, 4-spored, rarely 2-spored. Pleurocystidia absent. Cheilocystidia 32–75 × 4–10 × 4–6.8 × 4–11.2 µm; cylindrical, clavate, clavate-lageniform, or ventricose, sometimes subcapitate, septate. Pileipellis an ixocutis; epicutis 70–95 µm thick, tramal hyphae beneath subcutis angular, ellipsoid, sausage-shaped, inflating from septa ≤18 µm diam. Clamp connections occasionally present on cheilocystidia.

Specimen examined—TURKEY, **Hakkâri,** Şemdinli, Derya village, under *Quercus* sp., 37.3383°N 44.5322°E, 1616 m, 15.10.2018, Acar 1132 (VANF1132; GenBank MW544170, MW544171).

Phylogenetic results

Phylogenetic analyses were performed on the ITS dataset comprising 71 sequences, of which six were derived from our Turkish samples and two represented the outgroup. The 5′ and 3′ends were trimmed from the ~680 bp sequence alignment and of the 631 bp included in the final analysis, 130 were variable and 87 parsimony informative. Of the variable sites, the ITS1 possessed 72, the 5.8S gene only one, and the ITS2 57. BLAST and UNITE results of ITS sequences indicated 99% identity value for each sample.

Our Bayesian phylogenetic tree (Fig. 4) outlines the phylogenetic relationships and taxonomic positions among the species selected. Our *Hebeloma excedens* samples (VANF1051A,B) clustered with *H. excedens*, *H. mesophaeum*, and *H. subtortum* in *H.* sect. *Hebeloma* with strong support (PP = 0.97). The two *H. excedens* sequences grouped together with a PP = 1 value, expected because no nucleotide variation was observed between them. Differences between our and the database sequences were noted at ITS1 base 150 (C to T) and ITS2 base 530 T to C).

Our *Hebeloma geminatum* (VANF1116A, B) samples grouped closely with the database representatives in *H.* sect. *Denudata* (PP = 1), with *H. geminatum* closely related to *H. alpinum* (J. Favre) Bruchet, *H. aanenii* Beker & al., *H. crustuliniforme* (Bull.) Quél., *H. eburneum* Malençon, *H. salicicola* Beker & al., and *H. minus* Bruchet (Fig. 4). *Hebeloma geminatum* cannot be easily separated from its sister species based on ITS sequence data alone; here morphological characters are helpful. Eberhardt & al. (2015a) observed that a specimen almost certainly represents *H. geminatum* when the average width of the cheilocystidial apex exceeds 9 µm. The average cheilocystidial width in our material was 8–9 µm but its range extending to 11 µm supports its identification as *H. geminatum*.

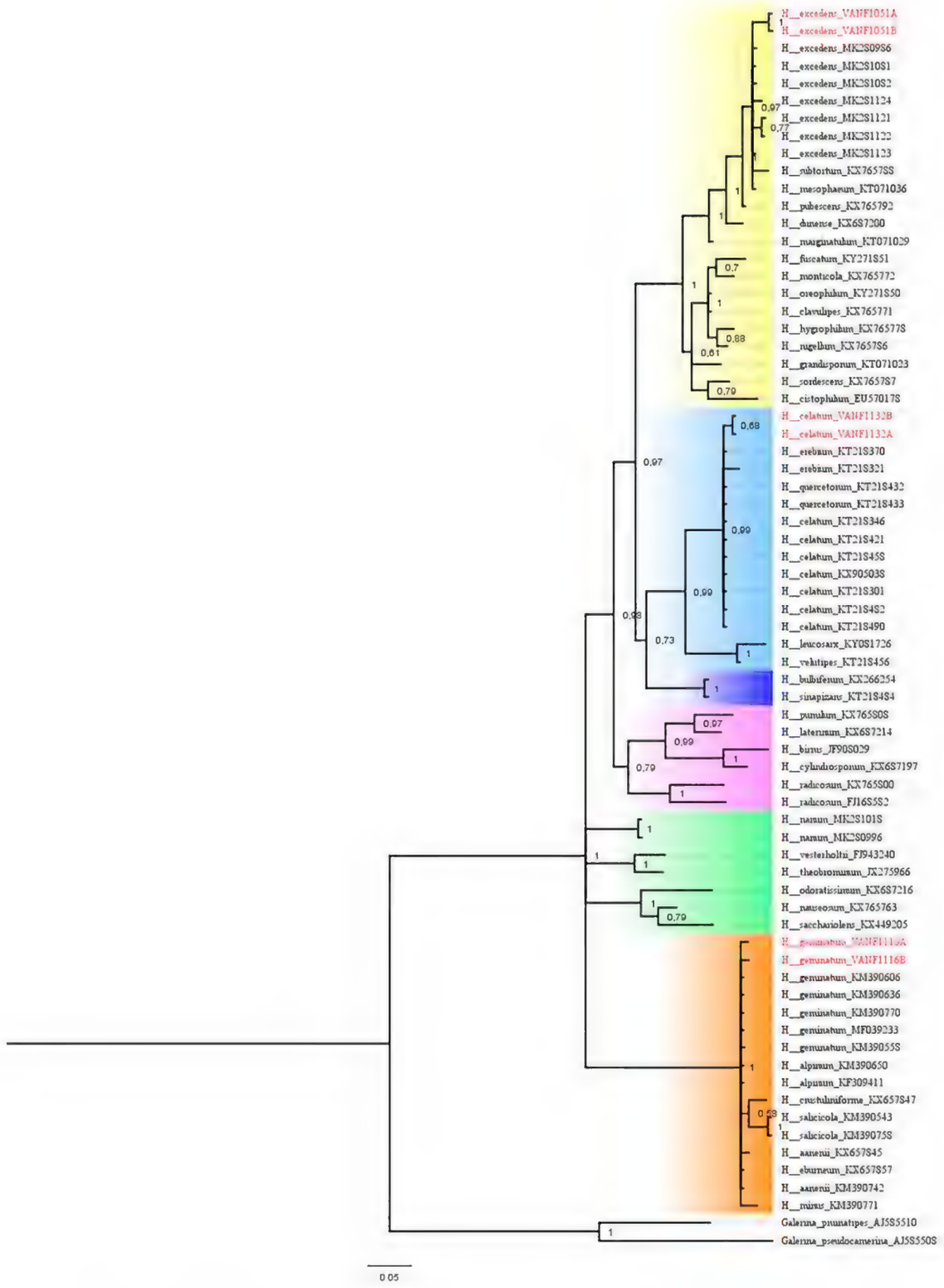

Fig 4. The Bayesian 50% majority rule consensus tree inferred from ITS region. PP> 0.5 are indicated above branches. Sequences from studied specimens are marked with red colour. *Hebeloma* sections are indicated with colours: yellow = *Hebeloma*, pale blue = *Velutipes*, dark blue = *Sinapizantia*, pink = *Scabrispora* & *Myxocybe*, green = *Sacchariolentia* & *Theobromina*, and orange = *Denudata*. Topology is rooted with *Galerina pseudocamerina* and *G. pruinatipes*.

Our *Hebeloma celatum* sequences (VANF1132A, B) clustered in *H.* sect. *Velutipes* (PP = 0.99) with *H. celatum, H. erebium* (Huijsman) Beker & U. Eberh., and *H. quercetorum* Quadr. (Fig. 4). This close phylogenetic relationship can be expected since these species are also morphologically very similar. Our *H. celatum* sequences were phylogenetically separated from representatives retrieved from the database due to nucleotide variations observed at base 497 (A to G).

Discussion

Hebeloma excedens and *Hebeloma geminatum* are recorded for the first time from Turkey, and *Hebeloma celatum,* previously reported for Turkey by Grilli & al. (2015), is confirmed for the country.

Hebeloma excedens and *H. mesophaeum* are not easily separated from each other because of their close morphological and ecological similarities. Nonetheless, the differences in pileus morphology are useful for distinguishing the species. The pileus of *H. excedens* is less yellow brown overall and less brown at the disc, and its margin extends over the lamellae. Also, *H. excedens* has fibrils on the stipe surface that are not observed in *H. mesophaeum* (Cripps & al. 2019, Beker & al. 2016). Our *H. excedens* material produced evenly coloured basidiomes that are more slender than customary for *H. mesophaeum* and cheilocystidia that are generally swollen at the base. Molecular data also supported subtle differences between the two species. Nucleotide variations observed at bases 453 (A to G) and 512 (C to T) support the two species as independent.

Hebeloma geminatum can be confused with *H. alpinum* and *H. aanenii.* Morphologically, the easiest way to separate *H. geminatum* from close relatives is through basidiospore and cheilocystidial comparison (Eberhardt & al. 2015a). The average basidiospore dimensions cited for *H geminatum* is <11 µm long and 6 µm diam. The basidiospores in our collections of *H. geminatum* measured 10–11.8 × 5.5–6.5 µm, while the cheilocystidia were generally swollen in the lower half but appeared spathulate. Eberhardt & al. (2015a) noted that they regarded specimens with cheilocystidial apices with an average width >9 µm to represent *H. geminatum;* our cheilocystidia measured ≤11 µm at the apex, meeting their morphological criterion. Molecular data supported this morphological identification, with nucleotide variations at bases 140 (G to A), 220 (indel), 562 (A to G) and 565 (G to A) bases separating *H. geminatum* from two close relatives.

Grilli & al. (2015) selected a large number of collections from throughout Europe to infer species diversity and evolutionary history in the two main *Hebeloma* sections, *Sinapizantia* and *Velutipes*. They included one *H. celatum* sample (KT218421) collected from Turkey in 2008 in their study, but as there was no mention of *H. celatum* in the Turkish mycobiota since then, we reevaluated *H. celatum* through morphological comparisons and molecular analyses. *Hebeloma celatum,* which produces mature basidiomes that greatly resemble those of *H. erebium* and *H. quercetorum,* can be distinguished by its floccose stem and raphanoid odor. More robust basidiomes with larger stipes help separate *H. celatum* from *H. erebium* (Grilli & al. 2015, Cripps & al. 2019), and the Turkish *H. celatum* specimens were robust. Likewise, the clearly clavate and sometimes subcapitate cheilocystidia distinguish our *H. celatum* from *H. quercetorum,* which is characterized by more regularly ventricose to cylindrical cheilocystidia. *Hebeloma celatum* associates with a variety of trees, among which the most commonly recorded is *Quercus* (Cripps & al. 2019); our specimens from Turkey were associated with *Quercus* species. Sequence variations at bases 140 (A to G) and 475 (A to G) also support separation of *H. celatum* from its two close relatives.

The above data well illustrate that macrofungal molecular analyses aid species identification and that the ITS region is particularly helpful in understanding the taxonomy and phylogeny of *Hebeloma.* Two *Hebeloma* species, *Hebeloma excedens* and *H. geminatum,* have been recorded as new for Turkey, increasing and the total species from twenty-eight to thirty. Moreover, our research confirmed the presence of *H. celatum* in Turkey.

Acknowledgements

This study was financially supported by Van Yüzüncü Yıl University (Scientific Research Project Foundation, FBA-2017-6132), Van, Turkey. We thank the Editor-in Chief Lorelei L. Norvell and Nomenclature Editor Shaun R. Pennycook for their critical reading and corrections. We also thank the pre-submission reviewers Dr Abdullah Kaya (Gazi University, Ankara, Turkey) and Dr Mustafa Emre Akçay (Van Yüzüncü Yıl University, Van, Turkey) for their valuable suggestions.

Literature cited

Aanen DK, Kuyper TW, Boekhout T, Hoekstra RF. 2000. Phylogenetic relationships in the genus *Hebeloma* based on ITS1 and 2 sequences, with special emphasis on the *Hebeloma crustuliniforme* complex. Mycologia 92: 269–281. https://doi.org/10.1080/00275514.2000.12061154

Aanen DK, Kuyper TW, Hoekstra RF. 2001. A widely distributed ITS polymorphism within a biological species of the ectomycorrhizal fungus *Hebeloma velutipes*. Mycological Research 105: 284–290. https://doi.org/10.1017/s0953756201003628

Beker HJ, Eberhardt U, Vesterholt J. 2016. *Hebeloma* (Fr.) P. Kumm. Fungi Europaei 14. Edizioni Technografica. 1218 p.

Cripps CL, Eberhardt U, Schütz N, Beker HJ, Evenson VS, Horak E. 2019. The genus *Hebeloma* in the Rocky Mountain Alpine Zone. MycoKeys 46: 1–54. https://doi.org/10.3897/mycokeys.46.32823

Dizkirici A, Acar A, Kalmer A, Uzun Y. 2019. Morphological and molecular characterization of *Hebeloma subtortum* (*Hymenogastraceae*), a new record macrofungus from Bingöl province, Turkey. Kastamonu Univ., Journal of Forestry Faculty 19(1): 1–10. https://doi.org/10.17475/kastorman.543375

Doğan HH, Kurt F. 2016. New macrofungi records from Turkey and macrofungal diversity of Pozantı-Adana. Turkish Journal of Botany. 40: 209–217. https://doi.org/10.3906/bot-1501-22.

Doyle JJ, Doyle JL. 1987. A rapid DNA isolation procedure for small quantities of fresh leaf tissue. Phytochemical Bulletin 19: 11–15.

Eberhardt U, Beker HJ, Vesterholt J, Dukik K, Walther G, Vila J, Fernández Brime S. 2012. European species of *Hebeloma* section *Theobromina*. Fungal Diversity 58(1): 103–126. https://doi.org/10.1007/s13225-012-0188-3

Eberhardt U, Beker HJ, Vesterholt J. 2015a. Decrypting the *Hebeloma crustuliniforme* complex: European species of *Hebeloma* section *Denudata* subsection *Denudata* (*Agaricales*). Persoonia 35: 101–147. https://doi.org/10.3767/003158515x687704

Eberhardt U, Ronikier A, Schütz N, Beker HJ. 2015b. The genus *Hebeloma* in the alpine belt of the Carpathians including two new species. Mycologia 107(6): 1285–1303. https://doi.org/10.3852/15-097

Grilli E, Beker HJ, Eberhardt U, Schütz N, Leonardi M, Vizzini A. 2015 ["2016"]. Unexpected species diversity and contrasting evolutionary hypotheses in *Hebeloma* (*Agaricales*) sections *Sinapizantia* and *Velutipes* in Europe. Mycological Progress 15(5): [46 p.]. https://doi.org/10.1007/s11557-015-1148-6

Güngör H, Solak MH, Allı H, Işıloğlu M, Kalmış E. 2015. New records for Turkey and contributions to the macrofungal diversity of Isparta Province. Turkish Journal of Botany 39: 867–877. https://doi.org/10.3906/bot-1406-28

Rambaut A. 2010. FigTree v1.3.1. Institute of Evolutionary Biology, University of Edinburgh, Edinburgh.

Ronquist F, Teslenko M, Mark PVD, Ayres DL. 2012. MrBayes 3.2: efficient Bayesian phylogenetic inference and model choice across a large model space. Systematic Biology 61: 539–542. https://doi.org/10.1093/sysbio/sys029

Sesli E, Denchev CM. 2014. Checklists of the myxomycetes, larger ascomycetes, and larger basidiomycetes in Turkey. 6th edn. Mycotaxon Checklists Online. 136 p. (http://www.mycotaxon.com/resources/checkl ists/sesli-v106-checklist.pdf).

Sesli E, Contu M, Vila J, Moreau PA, Battistin E. 2015. Taxonomic studies on some agaricoid and boletoid fungi of Turkey. Turkish Journal of Botany 39: 134–146. https://doi.org/10.3906/bot-1403-63.

Sesli E, Örtücü S, Aytaç E. 2018. Türkiye mikotası için yeni kayıtlar (*Basidiomycota Agaricales*). Bağbahçe Bilim Dergisi5(1): 15–20.

Solak MH, Işıloğlu M, Kalmış E, Allı H. 2015. Macrofungi of Turkey checklist (2nd ed.) Üniversiteliler Ofset, İzmir.

Tamura K, Stecher G, Peterson D, Filipski AM, Kumar S. 2013. MEGA 6: molecular evolutionary genetics analysis, version 6.0. Molecular Biology and Evolution 30(12): 2725–2729. https://doi.org/10.1093/molbev/mst197

Vesterholt J. 2005. The genus *Hebeloma*. Fungi of Northern Europe. Vol. 3. Svampetryk, Tilst, Denmark. 146 p.

Vesterholt J, Eberhardt U, Beker HJ. 2014. Epitypification of *Hebeloma crustuliniforme*. Mycological Progress 13: 553–562. https://doi.org/10.1007/s11557-013-0938-y

Wen J, Zimmer EA. 1996. Phylogeny and biogeography of *Panax* L. (the ginseng genus, *Araliaceae*): inferences from ITS sequences of nuclear ribosomal DNA. Molecular Phylogenetics and Evolution 6: 167–177. https://doi.org/10.1006/mpev.1996.0069

Yang Z, Rannala B. 1997. Bayesian phylogenetic inference using DNA sequences: a Markov chain Monte Carlo method. Molecular Biology and Evolution 14: 717–724. https://doi.org/10.1093/oxfordjournals.molbev.a025811